nor's Energy Advisory Council, The State of Texas (1974).
Rathore, R. N. S., K. A. VanWormer, and G. J. Powers, "Synthesis Strategies for Multicomponent Seqparation Systems with Energy Integration," *AIChE J.*, **20**, 491 (1974a).
Rathore, R. N. S., K. A. VanWormer, and G. J. Powers, "Synthesis of Distillation Systems with Energy Integration," *AIChE J.* **20**, 940 (1974b).
Reid, R. C., J. M. Prausnitz, and T. K. Sherwood, *The Properties of gases and liquids*, 3rd ed., McGraw Hill (1977).
Rodrigo, F. R., and J. D. Seader, "Synthesis of Separation Sequences by Ordered Branch Search," *AIChE J.*, **21**, 885 (1975).
Seader, J. C., and A. W. Westerberg, "A Combined Heuristic and Evolutionary Strategy for Synthesis of Simple Separation Sequences," *AIChE J.*, **23**, 951 (1977).
Siirola, J. J., "Progress toward the synthesis of heat integrated distillation schemes," paper 47a, 85th Nat. AIChE Mtg. Philadelphia (1978).
Siirola, J. J., G. J. Powers, and D. F. Rudd, "Synthesis of System Designs: III. Toward A Process Concept Generator," *AIChE J.*, **17**, 677 (1971).
Siirola, J. J., and D. F. Rudd, "Computer in Aided Synthesis of Chemical Process Designs; from Reaction Path Data to the Process Task Network," *Ind. Eng. Chem. Fundam.*, **10**, 353 (1971).
Sophos, A., G. Stephanopoulos, and M. Morari, "Synthesis of Optimum Distillation Sequences with Heat Integration Schemes," 71st Amn. AIChE Mtg., Miami (1978).
Stephanopoulos, G., and A. W. Westerberg, "Studies in Process Synthesis II; Evolutionary Synthesis of Optimal Process Flowsheets," *Chem. Eng. Sci.*, **31**, 195 (1976).
Stephanopoulos, G., and A. W. Westerberg, "The Use of Hestenes' Method of Multipliers to Resolve Dual Gaps in Engineering System Optimization," *J. Optim. Th. Appl.*, **15**, 285 (1975b).
Stupin, W. J., and F. J. Lockhart, "Thermally Coupled Distillation—A Case History," *Chem. Eng. Prog.*, **68**, 71 (Oct., 1972).
Tedder, D. W., and D. F. Rudd, "Parametric Studies in Industrial Distillation," *AIChE J.*, **24**, 303 (1978).
Umeda, T., K. Niida, and K. Shiroko, "A Thermodynamic Approach to Heat Integration in Distillation Systems," *AIChE J.*, **25**, 423 (1979).
Westerberg, A. W., "Decomposition Methods for Solving Steady State Process Design Problems," in *Decomposition of Large-Scale Problems*, D. M. Himmelblau, ed., North Holland (1973).
Westerberg, A. W., and G. Stephanopoulos, Letter to the Editors, *Chem. Eng. Sci.*, **31**, 325 (1976).
Westerberg, A. W., and G. Stephanopoulos, "Studies in Process Synthesis I; Branch and Bond Strategy with List Techniques for the Synthesis of Separation Schemes," *Chem. Eng. Sci.*, **30**, 963 (1975).
Wilde, D. J., and C. S. Beightler, *Foundations of Optimization*, Prentice Hall, Englewood Cliffs, N. J. (1967).

Manuscript received July 31, 1979; revision received November 28, and accepted January 25, 1980.

The Mixing of Granular Solids in a Rotary Cylinder

JACOB MU
and
D. D. PERLMUTTER
Department of Chemical
University of Pennsylvania
Philadelphia, Pennsylvania 19104

A model is derived for solids mixing and material transport in a continuous flow rotary dryer or reactor. Detailed analysis of the particle motions in the turnover process provides an opportunity to apply well-known reactor models to several subregions and to relate the overall results to different design geometries and operating conditions. The essential parameters of the model are the number of stages, the volume fractions of mixed flow and plug flow in each stage, the recycle ratio and the bypass ratio.

SCOPE

A new model is derived to describe in detail the particle movement patterns in various regions of a rotating cylinder such as find use as reactors, mixers and dryers. The solid feed rate, the speed of rotation and the effects of bed depth and cylinder geometry are included and accounted for. Tracer residence time distribution measurements and other bench scale experiments are suggested to estimate the parameters of the model.

CONCLUSIONS AND SIGNIFICANCE

A new model based on combinations of flow regimes in several subregions describes the isothermal mixing and the residence time distribution in a rotating cylinder. Comparisons are made with prior reports in the literature to emphasize the improvements expected and to demonstrate that the new model is applicable to a wide range of experimental conditions. This detailed phenomenological approach to the description of the mixing and transport processes uses sufficient details of the particle motions in each turnover step to be useful for the design of mixers, dryers and/or chemical reactors. Inclusion of appropriate thermal effects will be important, according to the purpose; this new model can also be extended to these applications.

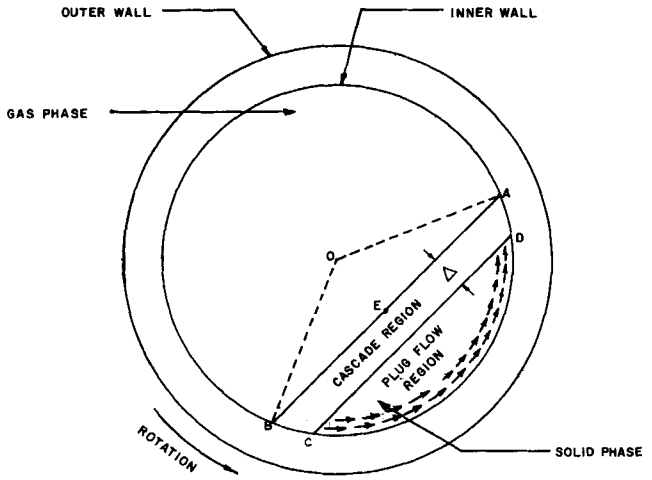

Figure 1. Geometry of rotary reactor cross section showing gas-solid interface and subregions within the solid bed.

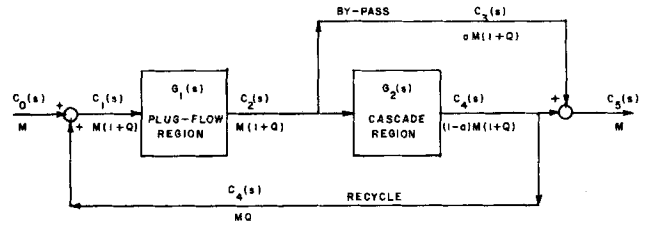

Figure 2. Block diagram for a single stage showing concentrations and flow quantities.

Rotary cylinder devices are used to handle large throughputs in physical processes for drying (Friedman and Marshall, 1949), size reductions (Davis, 1919; Erickson, 1953), agglomeration, mixing (Williams and Rahman, 1971), heating, cooling and solvent recovery, as well as for gas-solid chemical reaction and solid thermal decomposition (Wachters and Kramers, 1966; Szuniewicz and Manitius, 1974). Such devices are the geometry of preference when large throughput, surface renewal, charge mixing and controlled solid residence time are called for. The mixing operation of a rotary drum is favored by dispersion of solids both radially and longitudinally, but this effect should be minimized if the objective is to ensure a sufficiently homogeneous product. Further, the axial dispersion should be reduced to enhance thermal efficiency and obtain a uniform product from a rotary dryer or chemical reactor. It is therefore important in the design to be able to estimate the residence time distribution under various operating conditions.

The modeling of longitudinal dispersion for flow through tubular vessels was pioneered by Danckwerts (1953) and developed in many subsequent studies. Fan and Ahn (1961) used a similar unidirectional diffusion model to predict the dispersion and residence time distribution of solid material in a continuous rotary cylinder. Rutgers (1965) agreed that this model was adequate when uniform radial mixing was present and provided qualitative results for the effects of dimensions and speed of rotation on the dispersion. Abouzeid et al. (1974) adopted the same axial dispersion model to demonstrate its applicability but noted three explicit assumptions: material holdup is independ of axial position (axial velocity is constant), the radial mixing is large enough to smooth the concentration at any cross section and the dispersion coefficient is constant for fixed operating conditions. Wes et al. (1976) used the same approach and justified the axial dispersion model by noting the large Peclet number in their experimental system.

Although the axial dispersion model often provides an adequate description of particulate transport, it fails to account for changing axial velocity or changes in dispersion coefficient with position. Furthermore, there is reason to doubt that the radial mixing is necessarily much greater than that in the longitudinal direction. Above all, there is a need to carefully analyze each part of the turnover process to account for the details of mixing.

MODEL DEVELOPMENT

Following Rutgers (1965), the motions of particles in a rotary cylinder can be visualized as delineating two regions, as shown in Figure 1. The particles near the wall are carried in a direction opposite to the cascading layer, and there is no relative motion among them. When the particles reach the upper boundary of this region, they cascade down and mix with others. When rolling particles meet the wall, they move at random either downstream or upstream, producing a backmixing phenomenon that has been experimentally demonstrated. The particle movement associated with one complete turnover of the reactor can thus be described as following a plug flow pattern to the boundary of the cascade region, from where the particles assume a well-mixed flow with bypass. These behaviors are all combined in the block diagram of Figure 2, including recycle effects, but applicable at a selected cross section of the reactor.

Residence Time Distribution

If we adopt the block diagram notation shown in Figure 2, the transfer function for the plug flow region is

$$G_1(s) = \frac{C_2(s)}{C_1(s)} = e^{-\tau_1 s} \tag{1}$$

where

$$\tau_1 = \frac{M}{V}\left[\frac{1-P}{1+Q}\right] \tag{2}$$

The transfer function for the well-mixed cascade is

$$G_2(s) = \frac{C_4(s)}{C_2(s)} = \frac{1}{\tau_2 s + 1} \tag{3}$$

where

$$\tau_2 = \frac{V}{M}\left[\frac{P}{(1-a)(1+Q)}\right] \tag{4}$$

The ratio of output to input concentrations for the entire cross section may be expressed as

$$G(s) = \frac{C_5(s)}{C_0(s)} = \frac{(\tau_3 s + 1)e^{-\tau_1 s}}{(Q+1)(\tau_2 s + 1) - Qe^{-\tau_1 s}} \tag{5}$$

where

$$\tau_3 = \frac{VP}{M}\left[\frac{a}{1-a}\right] \tag{6}$$

If one assumes that the ratio P is the same through the cylinder, an N vessel series model can be applied to obtain

$$\frac{C_F(s)}{C_0(s)} = \frac{(\tau_3 s + 1)^N e^{-\tau_1 N s}}{[(Q+1)(\tau_2 s + 1) - Q e^{-\tau_2 s}]^N} \quad (7)$$

A polynomial expansion formula can be used to reduce Equation (7) to

$$\frac{C_F(s)}{C_0(s)} = \sum_{m=0}^{\infty} \sum_{k=0}^{N} B(m,k) e^{-\tau_1(m+N)s} (s + 1/\tau_2)^{-m-N+k} \quad (8)$$

where

$$B(m,k) = \frac{(N+m-1)!N^{m+1}}{(N-k)!k!m!} \left[\frac{Q^m}{(1+Q)^{N+m}}\right] \left[\tau_2^{-m+k-2N} \tau_3^k (\tau_2 - \tau_3)^{N-k}\right] \quad (9)$$

The response to specified inputs may be considered. If the forcing function is a step of size C_0

$$C_F(s) = \sum_{m=0}^{\infty} \sum_{k=0}^{N} \frac{C_0}{s} B(m,k) e^{-\tau_1(m+N)s} (s + 1/\tau_2)^{-m-N+k} \quad (10)$$

then the inverse Laplace transformation of $C_F(s)$ gives the dynamic response

$$C_F(t) = \sum_{m=0}^{\infty} \sum_{k=0}^{N} \frac{C_0 B(m,k)}{(m+N-k-1)!} \int_0^{t-\tau_1(m+N)} e^{-u/\tau_2} u^{m+N-k-1}\, du \quad (11)$$

If an impulse input of magnitude C_0 is used

$$C_F(s) = \sum_{m=0}^{\infty} \sum_{k=0}^{N} C_0 B(m,k) e^{-\tau_1(m+N)s} (s + 1/\tau_2)^{-m-N+k} \quad (12)$$

and the inverse time function gives the overall residence time distribution for the reactor as

$$E(t) = \frac{C_F(t)}{C_0} = \sum_{m=0}^{\infty} \sum_{k=0}^{N} \frac{B(m,k)}{(m+N-k-1)!} e^{-[t-\tau_1(m+N)]/\tau_2} [t - \tau_1(m+N)]^{m+N-k-1} \quad (13)$$

It should be noted in connection with the discussion of residence time distribution that the time of first breakthrough in such an experiment has particular significance since it is

$$t_0 = \tau_1 N \quad (14)$$

the sum of all the dead time contributions in N stages. Combining this observation with Equation (2) gives

$$Q = \frac{VN(1-P)}{Mt_0} - 1 \quad (15)$$

The parameters N (number of stages) and P (volume fraction of the cascade) are independently evaluated in the sections that follow. The value of Q (recycle ratio) can then be evaluated from Equation (15). This leaves only the bypass parameter a to be found by a best fit to the result of an experimental tracer study.

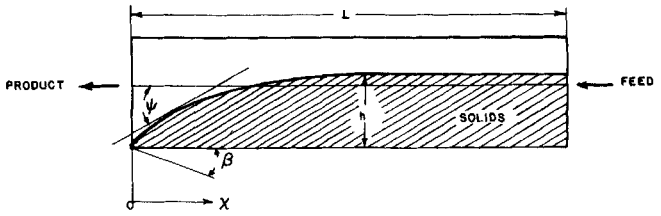

Figure 3. Geometry of rotary reactor length.

The Number of Turnover Stages

The number of equivalent stages in a rotating cylinder is the ratio of the overall average residence time to the time required for a single bed turnover:

$$N = \frac{T_0}{T} = \frac{FV_0/M}{\pi\phi_0/180\omega} \quad (16)$$

Because the solids level varies from inlet to exit, integrated averages are called for:

$$F = \int_0^1 f(x)\, d(x/L) \quad (17)$$

$$\phi_0 = \int_0^1 \phi(x)\, d(x/L) \quad (18)$$

At each axial position, ϕ is the sector angle occupied with solid material and f is the fraction of cylinder cross section that is filled. The geometry of Figure 1 gives this fraction as

$$f(x) = \frac{1}{2\pi}\left(\frac{\pi\phi}{180} - \sin\phi\right) \quad (19)$$

Combining Equations (17) and (19), we get

$$F = \frac{1}{2\pi}\int_0^1 \left(\frac{\pi\phi}{180} - \sin\phi\right) d\left(\frac{x}{L}\right) \quad (20)$$

and substituting Equations (18) and (20) into (16), we get a basis for comparison with experimental measurements:

$$N = \frac{90\omega V_0}{\pi^2 M} \frac{\int_0^1 \left(\frac{\pi\phi}{180} - \sin\phi\right) d\left(\frac{x}{L}\right)}{\int_0^1 \phi(x)\, d\left(\frac{x}{L}\right)} \quad (21)$$

However, detailed arguments are needed to relate ϕ to the geometry and operating parameters of the reactor. These are presented in the next section.

Solid Fill Levels

Saeman (1951) first derived the relationship between the mass flow in a rotating cylinder and the several significant angles illustrated in Figure 3. If attention is confined only to horizontal cylinders, $\beta = 0$ and the mass flow can be written in rigorous form as

$$M = \frac{(2/3)\omega R^3 \cot\theta \sin^3(\phi/2) \tan\psi}{\sqrt{1 + \cos^2\theta \tan^2\psi}} \quad (22)$$

The denominator term of Equation (22) differs from unity by less than 19% over the ranges of $0 \le \psi \le 40$ and $20 \le \theta \le 40$ deg. If such deviations are accepted, the rigorous relationship can be approximated by neglecting the denominator term to give

$$M = \frac{2}{3}\omega R^3 \cot\theta \sin^3(\phi/2) \tan\psi \qquad (23)$$

Equation (23) was used in turn by Saeman (1951), by Vahl and Kingma (1952) and by Kramers and Croockewit (1952). A closer approximation of Equation (22) can be formulated by using the substitution

$$\frac{\tan\psi}{\sqrt{1 + \cos^2\theta \tan^2\psi}} \simeq 2\tan(\psi/2) \qquad (24)$$

which provides errors less than 4% over the ranges of ψ and θ cited above. Substituting Equation (24) in Equation (22), we get

$$M = \frac{4}{3}\omega R^3 \cot\theta \sin^3(\phi/2) \tan(\psi/2) \qquad (25)$$

Hogg and Austin (1974) have suggested that a multiplicative factor be included in the formula for mass flow to account for the fractional time that a particle spends locked into the cascading motion. Yet other corrections are called for when the thickness of the cascade layer is appreciable in comparison with the total bed depth, since both the filling angle ϕ and the dynamic angle of repose θ are modified. If all the deviations from ideal flow are lumped into a single factor, Equation (25) becomes

$$M = \frac{4}{3}\omega\gamma R^3 \cot\theta \sin^3(\phi/2) \tan(\psi/2)$$
$$= 2K \tan(\psi/2) \sin^3(\phi/2) \qquad (26)$$

Substituting the half-angle formula, we get

$$M = 2K\sqrt{\frac{1-\cos\psi}{1+\cos\psi}} \sin^3(\phi/2) \qquad (27)$$

Rearranging, we get

$$\cos\psi = \frac{4K^2\sin^6\left(\frac{\phi}{2}\right) - M^2}{4K^2\sin^6\left(\frac{\phi}{2}\right) + M^2} \qquad (28)$$

From the geometry of Figure 3

$$\tan\psi = \frac{dh}{dx} = \frac{R}{2}\sin\left(\frac{\phi}{2}\right)\frac{d\phi}{dx} \qquad (29)$$

Combining Equations (28) and (29), we get

$$\frac{d\phi}{dx} = \frac{8KM\sin^2(\phi/2)}{R\left|\,4K^2\sin^6\left(\frac{\phi}{2}\right) - M^2\,\right|} \qquad (30)$$

The boundary condition needed in the integration of Equation (30) may be obtained from Saeman's observation that ψ must reduce to the static angle of repose at the exit end of the reactor; that is, $\psi=\theta_s$ at $x=0$, and from Equation (26)

$$\phi(0) = 2\sin^{-1}\left[\frac{M}{2K\tan(\theta_s/2)}\right]^{1/3} \qquad (31)$$

Integrating Equation (30) with boundary condition (31) provides an implicit solution for $\phi(x)$ needed in the computation of F by Equation (20) or N via Equation (21):

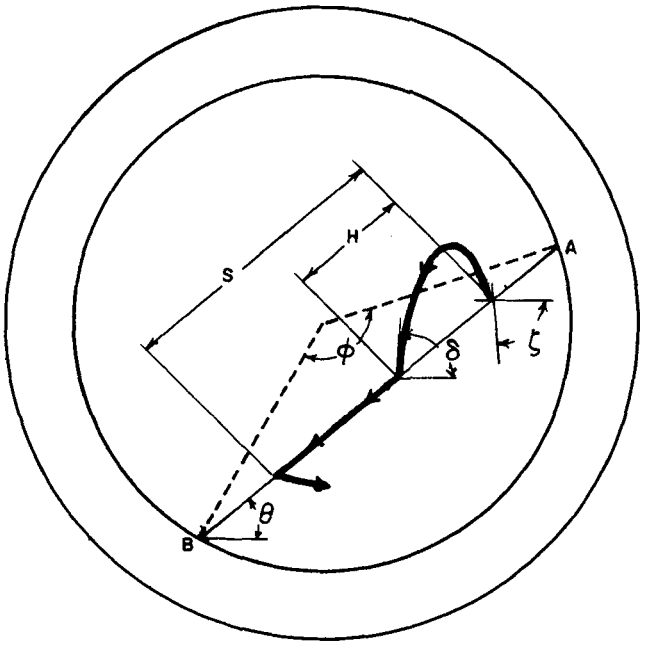

Figure 4. Geometry of particle trajectory.

$$\frac{2xM}{KR} = \int_{\phi(0)}^{\phi(x)} \frac{\left|\sin^6\left(\frac{\phi}{2}\right) - \left(\frac{M}{2K}\right)^2\right|}{\sin^2(\phi/2)} d\phi \qquad (32)$$

Cascade Volume

As noted with reference to Figure 1, the solids cross section may be divided into two subregions associated in this model with plug flow and well-stirred cascade, respectively. The cascade region occupies the area between the chords AB and CD

$$A_1 = \frac{R^2}{2}\left[\frac{\pi}{180}(\phi - 2\cos^{-1}r) - \sin\phi + 2r\sqrt{1-r^2}\right] \qquad (33)$$

where $r = [\cos(\phi/2) + \Delta/R]$. By subtracting both the cascade area and the triangle AOB from the sector, one may find the area of the plug flow segment:

$$A_2 = \frac{\pi R^2\phi}{360} - \frac{R^2\sin\phi}{2} - A_1 \qquad (34)$$

The fractional volume in the cascade is the ratio of the areas:

$$P = \frac{A_1}{A_1 + A_2} = \frac{\phi - 2\cos^{-1}r - \sin\phi + 2r\sqrt{1-r^2}}{\phi - \frac{180}{\pi}\sin\phi} \qquad (35)$$

Particle Trajectories

Individual particles are carried by the cylinder rotation to the surface of the solid layer from which point they assume either cascading or cataracting motion, depending on the speed of rotation. A generalization of this behavior is illustrated in Figure 4. The trajectory marked with arrows consists of a parabolic rise from the point of ejection to a maximum height, a parabolic fall to return to the solid surface, movement along the cascade surface and reentry into the bulk solid phase. As shown in Figure 4, the particle is ejected into the gas phase perpendicular to the radius of the cylinder at an angle to the horizontal

$$\zeta = 180 - \theta - \frac{\phi}{2} \tag{36}$$

with initial velocity components

$$v_x = \omega R \cos \zeta \tag{37}$$

and

$$v_w = \omega R \sin \zeta \tag{38}$$

The time of travel from ejection to maximum height is

$$t_1 = \frac{\omega R}{g} \sin \zeta \tag{39}$$

and the return from this height to the solid surface requires

$$t_2 = \frac{\omega R}{g} \sqrt{\sin^2\zeta + 4[\cos^2\zeta \tan\theta (\tan\theta + \tan\zeta)]} \tag{40}$$

Together, the particle has moved from its ejection point a distance of

$$H = \frac{2}{g}\left[\frac{(\omega R)^2 \cos^2\zeta (\tan\theta + \tan\zeta)}{\cos\theta}\right] \tag{41}$$

At the point of return, the particle strikes the cascading layer with velocity of magnitude

$$w = \sqrt{v_x^2 + (gt_2)^2} \tag{42}$$

at an angle to the horizontal of

$$\delta = \tan^{-1}(2 \tan\theta + \tan\zeta) \tag{43}$$

The impact produces an initial velocity component along the cascade surface of magnitude $w \cos(\delta-\theta)$. This initial vector is augmented by the acceleration of gravity and simultaneously retarded by friction with the inclined plane of the cascade surface. The net result is movement through the distance (S-H) over the time interval t_3, where

$$w \cos(\delta-\theta)t_3 + \frac{1}{2}g(\sin\theta - \mu\cos\theta)t_3^2 = S-H \tag{44}$$

Equation (44) provides an implicit solution for t_3 for any distance S and H.

At relatively low rotational speeds, the parabolic flight may take only a neglible time interval; however, the first term of Equation (44) must still be used to account for the initial velocity on the cascade. Under such conditions, $t_1=t_2=H=0$, and the average velocity of a particle along the cascade is

$$v(z) = \frac{S}{t_3} \tag{45}$$

depending only on the particle initial position expressed in terms of z, the fractional distance from point E to the wall along chord AB (Figure 1). At higher rotation rates, the averaging corresponding to Equation (45) would require the addition to numerator and denominator of the distances traveled along the parabolic arcs and their time intervals, respectively. At intermediate speeds of rotation, the parabolic arc will still be small, and the total distance traveled by a particle may be approximated by S. In this circumstance

$$v(z) = \frac{S}{t_1 + t_2 + t_3} \tag{46}$$

Surface Renewal Rate

Particles starting their cascade at different locations on the surface will follow different trajectories, since those that are initially close to the cylinder wall have larger initial velocities, proportional to their distances from the center of the cylinder. Moreover, the ensemble of particles that sequentially start from a given location will each follow a different path as they are randomly buffeted in the cascade. The detailed distribution of velocities is therefore unknown; it is nevertheless possible to find bounds on the average renewal velocities.

Because of the circular geometry of the cylinder cross section, the elements further from point E provide relatively greater contributions to the overall cascade as rotation sweeps out greater areas. The average velocity between E and the wall is

$$A = 2\int_0^1 z\, v(z)\, dz \tag{47}$$

Consider the case of complete segregation among the particle paths: each particle follows a fixed circular path through the solid, slides along the surface on a line having midpoint E and reenters the solid mass on the identical circular path as before. This configuration calls for

$$S = 2zR \sin\frac{\phi}{2} \tag{48}$$

and gives an upper bound for A because it provides the longest set of paths on the cascade consistent with the fixed turnover time. An alternative case is that of maximum mixedness in the cascade, where to preserve steady state each particle must travel the same distance along the cascade on each turnover, regardless of distance from E at any moment. In this circumstance

$$S = R \sin\frac{\phi}{2} \tag{49}$$

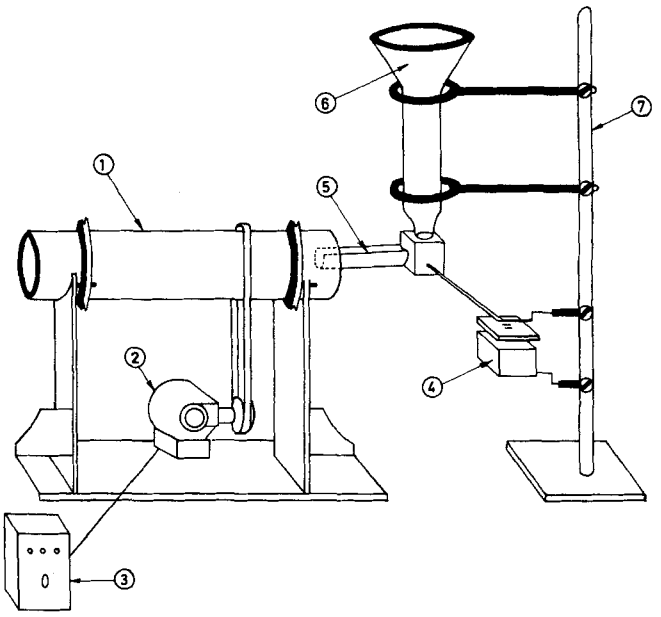

Figure 5. Schematic diagram of apparatus. 1. Rotary cylinder, 2. motor, 3. variable speed controller, 4. vibrator, 5. chute, 6. funnel, 7. support.

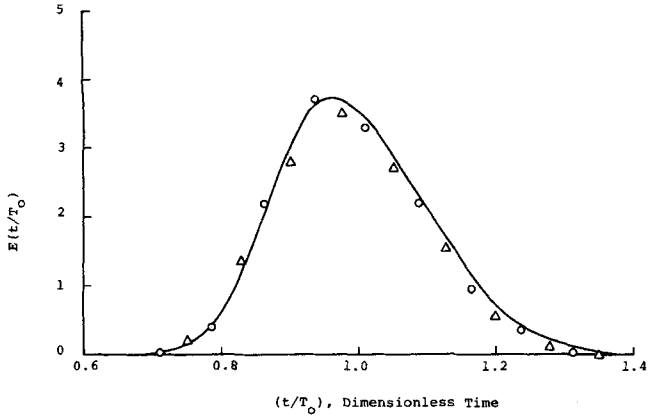

Figure 6. Residence time distribution: experimental points and best fit curve from model with $\tau = 0.55$ s, $\tau_2 = 1.61$ s, $\tau_3 = 1.37$ s.

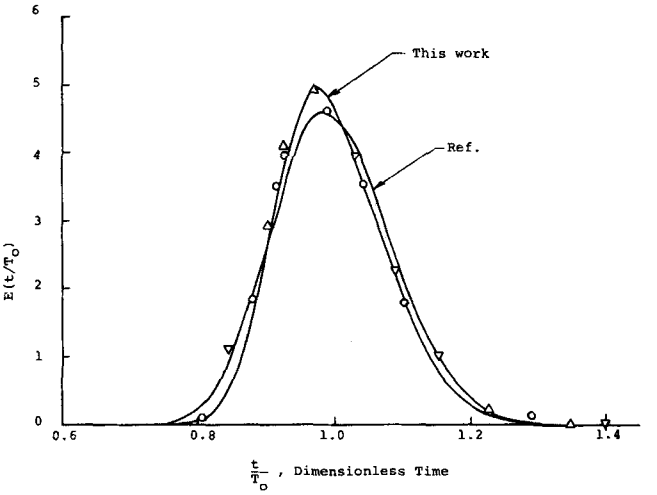

Figure 7. Residence time distribution of Abouzied (1974). Reference curve is from same source based on dispersion model. Fit of this work is computed with $\tau_1 = 0.340$ s, $\tau_2 = 1.89$ s, $\tau_3 = 1.76$ s.

and the average velocity A is a lower bound because the set of paths is cumulatively the shortest for a fixed turnover time.

When a value of A has been determined, the thickness of the cascade region can be estimated from

$$\Delta = \frac{\omega A_2}{60\pi A} \tag{50}$$

where A_2 is obtained from Equations (33) and (34).

EXPERIMENTAL

To test the correlative ability of the model under study, tracer experiments were run on a bench scale rotary cylinder to determine the residence time distribution of the particles fed. The equipment illustrated in Figure 5 was run at $n = 20$ rev/min and solid feed rate $M = 300$ cm³/min.

The apparatus consists of a horizontal plastic cylinder of 10.1 cm ID and 40.5 cm length, with inner wall covered with sandpaper to prevent slip of the rice particles used (2 mm diam. × 5 mm length). The solid feed rate is controlled by an oscillator with adjustable vibrating frequency. The constriction at the entrance is variable, but the discharge end is not constricted. When steady state was achieved, the experimental data included the dynamic angle of repose for the particles, as well as the feed rate and cylinder holdup volume under the test conditions.

An impulse input of 200 dyed particles was introduced and effluent samples were collected over 5 s intervals, 13 s apart. The impulse response was obtained by counting the dyed particles that emerged with each sample, and the resulting residence time distribution is presented as Figure 6. The circles and triangles are from duplicate runs needed to collect enough data for a smooth curve at the specified operating condition. It should be noted that the time scale of this figure has been normalized in the conventional manner by dividing by the average residence time T_0.

Table 1. Details of Calculations

		Data available	
Variable given	Symbol	From this experiment	From Abouzied (1974)
Cylinder radius, cm	R	5.08	4.0
Cylinder length, cm	L	40.6	24.0
Solid feed rate, cm³/min	M	300	85.7
Rotation speed, rev/min	n	20	42
Dynamic angle, deg	θ	35	40
Static angle, deg	θ_s	27	32
Particle material		Rice	Dolomite
		Results obtained	
Variable computed	Symbol	From this experiment	From Abouzied data
Geometric constant	K	15,684	13,418
Dimensionless feed rate of solids	(ML/KR)	0.153	0.0368
Solid bed angle at exit, deg	$\frac{\phi}{2}(0)$	20	57.0
Average fill fraction	F	0.122	0.190
Filled volume, cm³	V_0F	400	229
Average residence time, s	T_0	79.8	167
Average solid bed angle, deg	ϕ_0	98	119
Average surface renewal velocity cm/s	A	10.5	23
Cascade volume fraction	P	0.32	0.28
Breakthrough time, s	t_0	54	120
Recycle fraction	Q	0.01	0.01
Number of stages	N	98	353
Bypass fraction	a	0.84	0.93

The curve in Figure 6 is a best fit to the data. It was computed from Equation (13), which required numerical values of N, P, Q and a. All but the last of these parameters were available from the model equations, but a was found by trial. The details of these calculations are given in Table 1, showing the links between the experimental data and the more general model development.

DISCUSSION

To evaluate the proposed model with data from an independent source, a separate test was performed on literature data from Abouzeid (1974). Equation (16) was used to predict the average residence time for solids to be expected from Abouzeid's experimental system. This calculation gave 167 s as the average value, in very close agreement with Abouzeid's experimental determination of 170 s. In addition, the same data were used to estimate the four parameters of the new model presented here. For comparison, these computations are also summarized in Table 1, and the residence time distribution results are presented in Figure 7. The two curves in Figure 7 compare the data fits obtained with the model developed here and the conventional dispersion model. In this case, either model can correlate the data, but because the new model includes the details of the pattern of particle motions, it provides a way to account for point to point variations, especially if heats of reaction cause temperature inhomogeneities at any cross section.

The results of the two studies differ in the number of mixing stages N but are quite close with regard to the other three modeling parameters P, Q and a, demonstrating that the recycle and bypass characteristics of rotary reactors may be similar even when the number of effective stages is different. The bypass fraction is large and the recycle ratio is virtually negligible in both studies, but these characteristics may be expected to vary with rotation speed and geometry.

ACKNOWLEDGMENT

This research was funded by the U.S. Department of Energy, Office of Basic Energy Sciences under contract No. EY-76-S-02-2747.

NOTATION

a = fractional bypass in the cascading region
A = integrated average surface renewal velocity
A_1 = cross-sectional area of the cascade region
A_2 = cross-sectional area of the plug flow region
B = constant defined in Equation (9)
C_0 = concentration at inlet to a mixing stage
C_1 = concentration at extrance to the plug flow region
C_2 = concentration at exit from the plug flow region
C_4 = concentration at exit from the cascade region
C_5 = concentration in effluent from mixing stage
C_F = concentration in effluent from the reactor
$E(t)$ = residence time distribution of solids
f = fraction of cylinder cross section filled by solids
F = average solid filled fraction
g = gravitational constant
$G(s)$ = transfer function
h = depth of solid bed
H = distance between ejection point and point of return to cascade
k = index of summation in Equation (8)
K = constant defined in Equation (23)
L = total length of the rotary cylinder
m = index of summation in Equation (8)
M = volume flow rate of solids
n = speed of rotation
N = number of stages
P = volume fraction of cascade region
Q = recycle ratio in each mixing stage
R = radius of the rotary cylinder
s = Laplace transform parameter
S = total distance of travel along cascading layer
t = time
t_0 = time of breakthrough in residence time distribution experiment
t_1 = time of travel from ejection to maximum height
t_2 = time of travel from maximum height to return to cascade
t_3 = time of travel for movement along the solid surface
T = average residence time through the cylinder
T_0 = time for a single bed turnover
u = dummy time for integration
v = average surface renewal velocity for each particle
$v_x v_y$ = axial and vertical velocity component of the ejecting particle
V = total volume of the solid bed
V_0 = total volume of the rotary cylinder
w = speed of the particle striking the solid surface
x = distance measured along the rotary cylinder
z = fractional distance from point E to the wall along chord AB

Greek Letters

α = fractional conversion
β = inclination angle of the cylinder
τ = time constant
μ = coefficient of friction on the solid surface
ϕ = angle of sector occupied with solids
ϕ_0 = average angle of sector occupied with solid
ζ = angle to the horizontal of the ejecting particle
δ = angle to the horizontal of the striking particle
θ = dynamic angle of repose
θ_s = static angle of repose
ψ = angle of the solid surface relative to the axis of the cylinder
Δ = thickness of the cascading region
ω = angular rotation speed

LITERATURE CITED

Abouzeid, A.Z.M.A., T. S. Mika, K. V. Sastry, and D. W. Fuerstenau, "The Influence of Operating Variables on the Residence Time Distribution for Material Transport in a Continuous Rotary Drum," *Powder Technol.*, **10**, 273 (1974).

Danckwertz, P. V., "Continuous Flow Systems," *Chem. Eng. Sci.*, **2**, 1 (1953).

Davis, E. W., "Fine Crushing in Ball-Mills," *Trans. Am. Inst. Min. Metall. Engrs.*, **61**, 250 (1919).

Erickson, H. W., "Types of Grinding Mills and When to Use Them," *Chem. Eng. Progr.*, **49**, 63 (1953).

Fan., L. T., and Y. K Anh, "Axial Dispersion of Solids in Rotary Solid Flow Systems," *Appl. Sci. Res.*, **A10**, 465 (1960).

Friedman, S. J., and W. R. Marshall, "Studies in Rotary Drying," *Chem. Eng. Progr.*, **45**, 480 (1949).

Hogg, R., K. Shoki, and L. G. Austin, "Axial Transport of Dry Powders in Horizontal Rotating Cylinders," *Powder Technol.*, **8**, 99 (1974).

Kramers, H., and P. Croockewit, "The Passage of Granular Solids Through Inclined Rotary Kilns," *Chem. Eng. Sci.*, **1**, 259 (1952).

Rutgers, R., "The Longitudinal Mixing of Granular Materials in a Rotary Cylionder," *ibid.*, **20**, 1079 (1965).

Seaman, W. C., "Passage of Solids Through Rotary Kilns," *Chem. Eng. Prog.*, **47**, 508 (1951).

Szuniewicz, R., and H. Manitius, "Mathematical Model of the Aluminum Oxide Rotary Kiln," *Chem. Eng. Sci.*, **29**, 1701 (1974).

Vahl, L., and W. G. Kigma, "Transport of Solids Through Horizontal Rotary Cylinders," *ibid.*, **1**, 253 (1952).

Wachters, L. H. J., and H. Kramers, "The Calcining of Sodium Bicarbonate in a Rotary Kiln," *Symp. Two Phase Flow, Proc.* **1**, 501 (1966).

Wes, G. W. J., A. A. H. Drinkenburg, and S. Stemerding, "Solids Mixing and Residence Time Distribution in a Horizontal Rotary Drum Reactor," *Powder Technol.*, **13**, 177 (1976).

Williams, J. C., and M. A. Rahman, "Prediction of the Performance of Continuous Mixers for Particulate Solids Using Residence Time Distributions," *ibid.*, **5**, 87 (1971)

Manuscript received April 21, 1978; revision received April 11, and accepted December 10, 1979.